Identification and Characterization of a Divalent Metal Ion-Dependent Cleavage Site in the Hammerhead Ribozyme †

ARTICLE *in* BIOCHEMISTRY · DECEMBER 2001

Impact Factor: 3.02 · DOI: 10.1021/bi015634c · Source: PubMed

3 AUTHORS, INCLUDING:

Frédéric Godde
Université Bordeaux 1
18 PUBLICATIONS **486** CITATIONS
SEE PROFILE

Snorri Th Sigurdsson
University of Iceland
113 PUBLICATIONS **2,820** CITATIONS
SEE PROFILE

Identification and Characterization of a Divalent Metal Ion-Dependent Cleavage Site in the Hammerhead Ribozyme†

John C. Markley, Frédéric Godde,‡ and Snorri Th. Sigurdsson*

Department of Chemistry, University of Washington, Seattle, Washington 98195-1700

Received August 1, 2001; Revised Manuscript Received September 14, 2001

ABSTRACT: We describe a new RNA cleavage motif, found in the hammerhead ribozyme. Cleavage occurs between nucleotides G8 and A9, yielding a free 5′-hydroxyl group and a 2′,3′-cyclic phosphate. This cleavage is dependent upon divalent metal ions and is the first evidence for a metalloribozyme known to show preference for Zn^{2+}. Cleavage is also observed in the presence of Ni^{2+}, Co^{2+}, Mn^{2+}, Cd^{2+}, and Pb^{2+}, while negligible cleavage was detected in the presence of the alkaline-earth metal ions Mg^{2+}, Ca^{2+}, Sr^{2+}, and Ba^{2+}. A linear relationship between the logarithm of the rate and pH was observed for the Zn^{2+}-dependent cleavage, which is indicative of proton loss in the cleavage mechanism, either prior to or in the rate-determining step. We postulate that a zinc hydroxide complex, bound to the known A9/G10.1 metal ion binding site, abstracts the proton from the 2′-hydroxyl group of G8, which attacks the A9 phosphate and initiates cleavage. This hypothesis is supported by a previously reported crystal structure [Murray, J. B., Terwey, D. P., Maloney, L., Karpeisky, A., Usman, N., Beigelman, L., and Scott, W. G. (1998) *Cell 92*, 665−673], which shows the conformation required for RNA cleavage and proximity of the 2′-hydroxyl group to the metal ion complex.

The hammerhead ribozyme (Figure 1A) is an RNA motif that catalyzes the cleavage of an RNA substrate via a transesterification reaction, producing a 2′,3′-cyclic phosphate and a 5′-hydroxyl terminus (Figure 1B) (*1*). Divalent metal ions have been implicated directly in the hammerhead ribozyme cleavage mechanism (*2*−*5*), and the most popular mechanism has involved the abstraction of the 2′-hydroxyl proton at the cleavage site by a metal ion hydroxide (*6*). Divalent metal ions can also play a structural role in ribozyme activity by stabilizing the catalytically active tertiary conformation through coordination to heteroatoms, such as oxygen atoms or nitrogen atoms present in the nucleoside bases. The finding that the hammerhead ribozyme is active in the absence of divalent metal ions at high concentrations of monovalent metal ions calls into question the role of divalent metal ions in the mechanism of substrate cleavage (*5*, *7*, *8*).

Divalent metal ion binding sites in the hammerhead ribozyme have been found by X-ray crystallography (*9*−*13*) and by NMR spectroscopy (*14*). One of the most extensively studied metal ion binding sites is the A9/G10.1 site which involves coordination of the metal ion to N7 of G10.1 and the *pro*-R_P phosphate oxygen of A9 (Figure 2). The *pro*-R_P oxygen of A9 has been implicated in hammerhead ribozyme function by replacement of the nonbridging, *pro*-R_P oxygen at the A9 phosphate with sulfur. Substrate cleavage studies in the presence of Mg^{2+} resulted in reduced

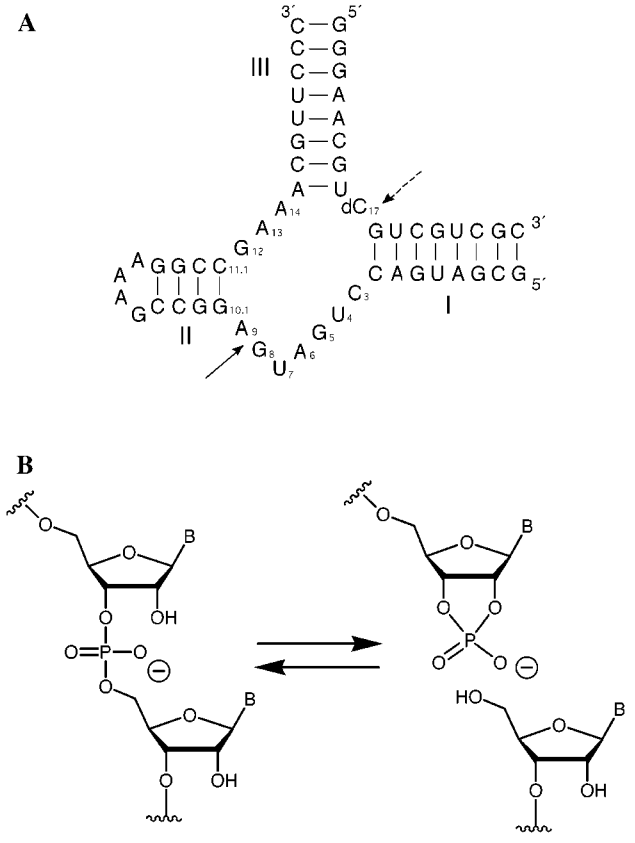

FIGURE 1: (A) Primary and secondary structure of the hammerhead ribozyme shown annealed to a noncleavable substrate. The dashed arrow denotes the substrate cleavage site. The solid arrow denotes the ribozyme cleavage site. Roman numerals represent the three helical regions. (B) Transesterification of an RNA phosphodiester bond.

† This work was supported by a grant from the National Institutes of Health (GM56947).

* Corresponding author. E-mail: sigurdsson@chem.washington.edu.

‡ Present address: Institut Européen de Chimie et Biologie, 16 Av. Pey Berland, 33607 PESSAC Cedex, France.

10.1021/bi015634c CCC: $20.00
Published on Web 10/20/2001

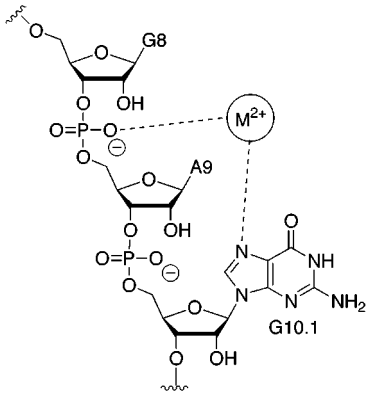

FIGURE 2: A9/G10.1 metal ion binding site in the hammerhead ribozyme. A divalent metal ion is shown bound to the N7 of G10.1 and the *pro-*R_P phosphate oxygen of A9.

ribozyme activity, but activity was restored by replacing Mg^{2+} with the more thiophilic Mn^{2+} ion (*15*). The N7 atom of G10.1 was also shown to be important for hammerhead ribozyme activity by replacement of G10.1 with 7-deazaguanosine (*16*). The metal ion bound to the A9/G10.1 site has also been directly linked to substrate cleavage (*17*, *18*), although this is currently disputed (*19*).

We describe here the catalytic properties of A9/G10.1-bound divalent metal ions in the hammerhead ribozyme toward the specific cleavage of the phosphodiester bond between nucleotides G8 and A9, yielding termini containing a 2′,3′-cyclic phosphate and a 5′-hydroxyl (Figure 1B). We also show that this cleavage activity does not require the full-length sequence of the hammerhead ribozyme. To our knowledge, this RNA cleavage motif is the first ribozyme activity that shows a preference for zinc ions.

MATERIALS AND METHODS

General. Commercial reagents and solvents were used as received. Monosodium salts of MES,[1] MOPS, HEPES, TAPS, and CHES, disodium salts of PIPES and EDTA, imidazole, and piperidine were from Sigma Chemical Co. Urea, Tris, and boric acid were from Angus Chemical Co. Aqueous solutions of 40% w/v 19/1 w/w acrylamide/*N*,*N*′-methylenebis(acrylamide) were from Bio-Rad. Formamide, bromphenol blue, xylene cyanole FF, 1 M tetrabutylammonium fluoride (TBAF) in tetrahydrofuran (THF), LiCl, NaCl, $Ca(OAc)_2$, $Cd(OAc)_2$, $Cu(OAc)_2$, $Pb(OAc)_2$, and $Sr(OAc)_2$ were from Aldrich Chemical Co. $Ba(OAc)_2$ and $Ni(OAc)_2$ were from J. T. Baker Chemical Co. $Hg(OAc)_2$ and $Mg(OAc)_2$ were from Allied Chemical Co. $Co(OAc)_2$ was from Mallinckrodt Chemical Works. $Mn(OAc)_2$ was from Avocado Research Chemicals, Ltd. $Zn(OAc)_2$, MeOH, and aqueous HCl were from Fisher Scientific Chemical Co. H_2O was purified on a Millipore Milli-Q Water System and used in all aqueous solutions. Buffers, aqueous NaCl, and H_2O were autoclaved. $M(OAc)_2$ (500 or 250 mM) solutions were freshly prepared using sterilized water.

Oligomer concentrations were calculated using a molar extinction coefficient (ϵ_{260}) of 3.706×10^5, 1.623×10^5, 1.835×10^5, and 2.267×10^5 L mol^{-1} cm^{-1} for the ribozyme, noncleavable substrate, short ribozyme subsequence (U7−A14), and chimeric oligonucleotide, respectively.

Mass spectrometric analysis of oligonucleotides was performed on an Esquire-LC electrospray ion trap mass spectrometer (Bruker/Hewlett-Packard) in the negative ion mode. The oligonucleotide (1 nmol) was diluted to a final concentration of 5 mM imidazole, 5 mM piperidine, 20 μM oligomer, and 1/9 v/v MeOH/H_2O. The imidazole/piperidine buffer was used to minimize alkaline metal adducts (*20*). The sample was injected at 1 μL/min via a syringe pump. Molecular weights were determined from spectra of multiply charged ions by deconvolution using Bruker DataAnalysis (version 1.6m) software.

Oligonucleotide purification and analyses of cleavage experiments were performed on 20% denaturing polyacrylamide gels containing 7 M urea, 90 mM Tris, 90 mM boric acid, and 1 mM Na_2EDTA. For the cleavage experiments, the bands were visualized by phosphorimaging (Molecular Dynamics 400A PhosphorImager) and analyzed using Molecular Dynamics ImageQuant (version 5.1) software.

Preparation of Ribozyme and Noncleavable Substrate. Hammerhead ribozyme, noncleavable substrate, and a short ribozyme subsequence (U7−A14) were purchased from Dharmacon Research, Inc., and deprotected using reagents and conditions provided (*21*). For preparation of 5′-^{32}P-labeled oligonucleotides, a solution containing the oligomer (2 nmol) in H_2O (11.5 μL) and 10 × forward reaction buffer (2.5 μL, Promega) was treated with T4 polynucleotide kinase (10 units, 1 μL, Promega) and [γ-^{32}P]ATP (10 μCi/μL, 10 μL, NEN Life Science Products). The solution was incubated at 37 °C for 45 min followed by addition of 8 M urea containing 0.25% w/v bromphenol blue (50 μL). The solution was incubated at 60 °C for 2 min and then purified by denaturing polyacrylamide gel electrophoresis (DPAGE). The band of purified oligomer was visualized by exposure to X-ray film (5 min, Fuji), excised, crushed, and eluted from the gel with 10 mM Tris, 1 mM Na_2EDTA, 250 mM NaCl, pH 7.5 (5 mL), overnight at 4 °C. The gel particles and supernatant were separated by centrifugation, and the supernatant was removed, filtered (0.45 μm nylon, Alltech), and desalted on a Sep-Pak C_{18} Classic Cartridge (Waters) (*22*). For preparative purification of the ribozyme and noncleavable substrate, the oligomers (250 nmol) were purified by DPAGE, visualized by UV-shadowing, isolated, and desalted as described above.

Preparation of Chimeric Oligonucleotide. The chimeric oligonucleotide 5′-CGA ACT CAC TAT (rA)GG AAG AGA TG, containing deoxynucleotides with the exception of a single ribonucleotide (*23*), was synthesized with an Applied Biosystems 394 automated DNA/RNA synthesizer on a 1 μmol scale using standard DNA phosphoramidites (CPG) and 2′-*tert*-butyldimethylsilyl-protected A phosphoramidite (CPG). The solid support-bound oligonucleotide was deprotected in concentrated NH_4OH at 55 °C for 16 h followed by concentration of the supernatant to dryness in vacuo. The resulting residue was dissolved in 1 M TBAF in THF (0.5

[1] Abbreviations: ATP, adenosine triphosphate; CHES, 2-(*N*-cyclohexylamino)ethanesulfonic acid; DPAGE, denaturing polyacrylamide gel electrophoresis; EDTA, ethylenediaminetetraacetic acid; ESIMS, electrospray ionization mass spectrometry; HEPES, *N*-(2-hydroxyethyl)-piperazine-*N*′-2-ethanesulfonic acid; MES, 2-(*N*-morpholino)ethanesulfonic acid; MOPS, 3-(*N*-morpholino)propanesulfonic acid; PIPES, piperazine-*N*,*N*′-bis(2-ethanesulfonic acid); TAPS, *N*-tris(hydroxymethyl)methyl-3-aminopropanesulfonic acid; TBAF, tetrabutylammonium fluoride; THF, tetrahydrofuran; Tris, tris(hydroxymethyl)aminomethane; UV, ultraviolet.

mL) and incubated at 37 °C for 16 h followed by addition of 1 M Tris, pH 7.4 (0.5 mL). The solution was then concentrated in vacuo to ca. 0.4 mL and desalted on a NAP-10 G25 Sephadex column (Amersham Pharmacia). The RNA was eluted with 10 mM Tris, 1 mM Na_2EDTA, pH 7.5 (1.5 mL), and concentrated to dryness in vacuo. The crude oligonucleotide was purified by DPAGE, visualized by UV-shadowing, eluted from the gel, filtered, and desalted on a Sep-Pak as above. ESIMS: observed ions (*m*/*z*) 617.8 (11^-), 679.6 (10^-), 755.5 (9^-), 849.9 (8^-), 971.2 (7^-), 1133.2 (6^-). Average MW: 6806.8, std dev: 1.0 (calcd 6808.5).

Determination of Cleavage Products. Unlabeled ribozyme (5 nmol), 500 mM MOPS, pH 7.1 (pH at 37 °C, 10 μL), 1 M NaCl (15 μL), and 500 μM Na_2EDTA (2 μL) were combined and concentrated to dryness in vacuo. The residue was dissolved in H_2O (80 μL), heated at 60 °C for 2.5 min, and cooled to ambient temperature. Cleavage was initiated by addition of 500 μM $Zn(OAc)_2$ (20 μL). Final concentrations (100 μL): 50 mM MOPS, 10 μM Na_2EDTA, 200 mM Na^+, 50 μM ribozyme, and 100 μM $Zn(OAc)_2$. The reaction was performed at 37 °C for 6 days (144 h). The solution was then desalted with a Sep-Pak as described above. The cleavage products were dissolved in H_2O (50 μL) and quantified by UV. Approximately 1 nmol of each product was analyzed by mass spectrometry as described above. ESIMS 5′-cleavage product: observed ions (*m*/*z*) 648.8 (7^-), 757.1 (6^-), 908.6 (5^-), 1136.1 (4^-). Average MW: 4548.6, std dev: 0.4 (calcd 4547.7). ESIMS 3′-cleavage product: observed ions (*m*/*z*) 592.3 (13^-), 641.7 (12^-), 700.4 (11^-), 770.3 (10^-), 856.0 (9^-), 963.2 (8^-). Average MW: 7713.3, std dev: 1.0 (calcd 7712.8).

Time Course of Zn^{2+}-Promoted Cleavage. For time course experiments involving the ribozyme, 500 mM buffer (10 μL), 500 μM Na_2EDTA (2 μL), 1 M NaCl (10, 15, or 20 μL, depending on Na^+ content of buffer), 40 μM noncleavable substrate (5 μL), and the ^{32}P-labeled ribozyme (trace amounts) were combined and concentrated to dryness in vacuo. The residue was dissolved in H_2O (80 μL), incubated at 60 °C for 2.5 min, cooled to ambient temperature, and treated with either H_2O (20 μL) for the control experiments or 500 μM $Zn(OAc)_2$ (20 μL). Final concentrations (100 μL): 50 mM buffer, 10 μM Na_2EDTA, 200 mM Na^+, 2 μM noncleavable substrate, <300 nM ribozyme, and 0 or 100 μM $Zn(OAc)_2$. Reactions were performed at 37 °C for 3 (pH 8.1−9.1), 6 (pH 7.1−7.7), or 11 (pH 5.6−6.5) days. Time points were taken (5 μL) to which was added stop mix (24/1 v/v formamide/10 mM Na_2EDTA, 5 μL). Reactions were stored at −20 °C until analysis by DPAGE. For time course experiments involving the chimeric oligonucleotide or short ribozyme subsequence (U7−A14), conditions were the same as described for the ribozyme except that the noncleavable substrate was left out of the reaction solution.

Divalent Metal Ion Screening. Tris (500 mM), pH 8.6 (pH at 37 °C, 25 μL), 1 mM Na_2EDTA (2.5 μL), 1 M NaCl (50 μL), 261 μM noncleavable substrate (1.91 μL), and ^{32}P-labeled ribozyme (trace amounts) were combined and concentrated to dryness in vacuo. The residue was dissolved in H_2O (200 μL), heated at 60 °C for 2.5 min, cooled to ambient temperature, and aliquoted (4 μL) to microtubes. The solutions were treated with either H_2O (1 μL) for the control experiment or a 100 μM solution of the diacetates of Ba^{2+}, Ca^{2+}, Cd^{2+}, Co^{2+}, Cu^{2+}, Hg^{2+}, Mg^{2+}, Mn^{2+}, Ni^{2+}, Pb^{2+}, Sr^{2+}, or Zn^{2+} (1 μL). Final concentrations (5 μL): 50 mM Tris, 10 μM Na_2EDTA, 200 mM NaCl, 2 μM noncleavable substrate, <300 nM ribozyme, and 0 or 20 μM $M(OAc)_2$. Reactions were performed at 37 °C for 24 h. Reactions were stopped by adding stop mix (5 μL) and stored at −78 °C until analysis by DPAGE.

Li^+/Na^+-Zn^{2+} Competition Experiment. Tris (500 mM), pH 7.6 (pH at 37 °C, 25 μL), 1 mM Na_2EDTA (2.5 μL), 1 M LiCl or NaCl (0−20 μL), 261 μM noncleavable substrate (1.91 μL), and ^{32}P-labeled ribozyme (trace amounts) were combined and concentrated to dryness in vacuo. The residue was dissolved in H_2O (200 μL), heated at 60 °C for 2.5 min, cooled to ambient temperature, and aliquoted (4 μL) to microtubes. The solutions were treated with either H_2O (1 μL) for the control experiments or 500 μM $Zn(OAc)_2$ (1 μL). Final concentrations (5 μL): 50 mM Tris, 10 μM Na_2EDTA, 0−5 M LiCl or NaCl, 2 μM noncleavable substrate, <300 nM ribozyme, and 0 or 100 μM $Zn(OAc)_2$. Reactions were performed at 37 °C for 24 h. Reactions were stopped by adding stop mix (5 μL) and stored at −20 °C until analysis by DPAGE.

$Mg^{2+}-Zn^{2+}$ Competition Experiment. Tris (500 mM), pH 8.6 (pH at 37 °C, 17 μL), 1 mM Na_2EDTA (1.7 μL), 1 M NaCl (34 μL), 261 μM noncleavable substrate (1.30 μL), and ^{32}P-labeled ribozyme (trace amounts) were combined and concentrated to dryness in vacuo. The residue was dissolved in H_2O (102 μL), heated at 60 °C for 2.5 min, cooled to ambient temperature, and aliquoted (6 μL) to microtubes. The solutions were treated with either H_2O (2 μL) for the control experiments or 5 μM−500 mM $Mg(OAc)_2$ (2 μL). The solutions were incubated at ambient temperature for 15 min followed by the addition of H_2O (2 μL) for the control experiments or 500 mM $Zn(OAc)_2$ (2 μL). Final concentrations (10 μL): 50 mM Tris, 10 μM Na_2EDTA, 200 mM NaCl, 1 μM−100 mM $Mg(OAc)_2$, 2 μM noncleavable substrate, <300 nM ribozyme, and 0 or 100 μM $Zn(OAc)_2$. Reactions were performed at 37 °C for 24 h. Reactions were stopped by adding stop mix (10 μL) and stored at −20 °C until analysis by DPAGE.

RESULTS

Identification of the Cleavage Site. Zn^{2+}-dependent cleavage between G8 and A9 was serendipitously observed during experiments unrelated to this study. To further investigate this new cleavage site, we chose a well-characterized construct of the hammerhead ribozyme, referred to as HH16 (*24*), and a noncleavable substrate containing a deoxynucleotide at the cleavage site (Figure 1). A trace amount of 5′-^{32}P-labeled ribozyme was used and substrate concentration held at 2 μM in order to ensure ribozyme−substrate complex formation. Initially, specific cleavage was observed between nucleotides G8 and A9 in the absence of Zn^{2+} (data not shown), presumably due to the presence of trace amounts of divalent metal ion contaminants. This contaminant-dependent cleavage was completely suppressed at 10 μM EDTA (data not shown).

Determination of Cleavage Position and Identity of Cleavage Products. The site of Zn^{2+}-promoted cleavage in the hammerhead ribozyme was determined to be between G8 and A9 by T1 RNase digestion and DPAGE analysis (data not shown). The cleavage position was verified, and

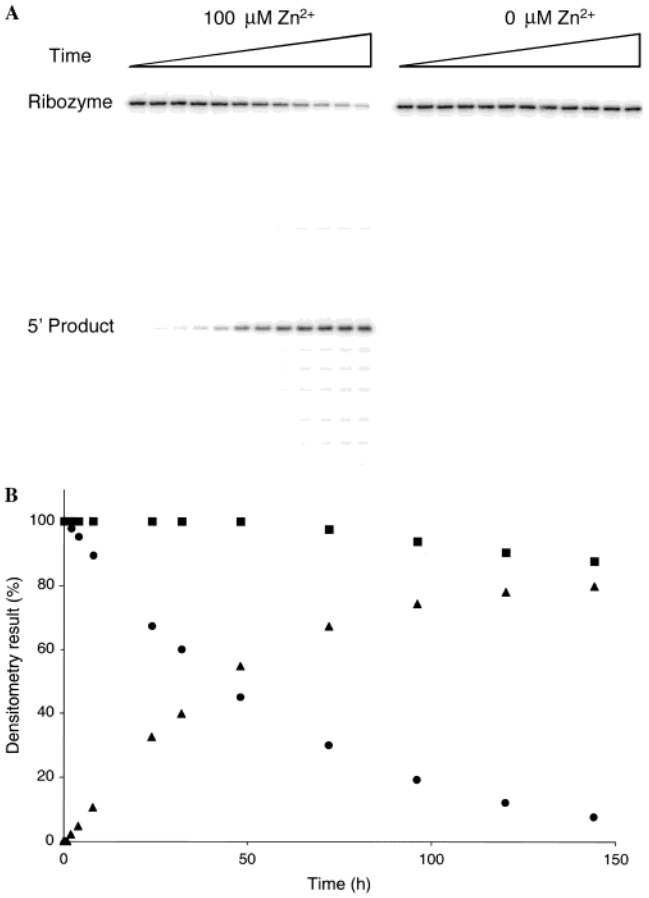

FIGURE 3: (A) Time course of Zn^{2+}-promoted cleavage. Conditions (37 °C, 144 h): 50 mM MOPS, pH 7.1, 200 mM Na^+, 10 μM Na_2EDTA, 2 μM noncleavable substrate, <300 nM ribozyme, 0 or 100 μM $Zn(OAc)_2$. (B) Plot showing the disappearance of full-length ribozyme (circles), the appearance of G8/A9 cleavage product (triangles), and the sum of the full-length ribozyme and the cleavage product (squares).

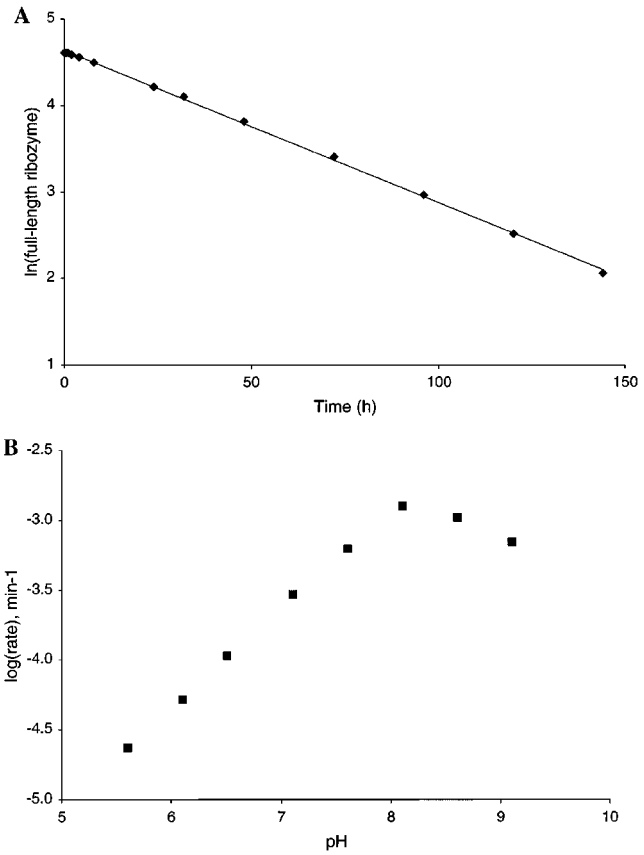

FIGURE 4: (A) Determination of the rate of cleavage at pH 7.1 by plotting the natural logarithm of the percent full-length ribozyme remaining as a function of time. (B) pH dependence on the Zn^{2+}-promoted cleavage rate.

the resulting termini were characterized by mass spectrometry. Interestingly, the noncleavable substrate was found to have only a small effect on the extent of cleavage and was therefore left out to simplify the mass spectrum. Deconvolution of the multiply charged ions in the mass spectrum revealed two oligonucleotides corresponding to cleavage between nucleotides G8 and A9, resulting in a 2′,3′-cyclic phosphate and a 5′-hydroxyl terminus. Furthermore, an oligonucleotide containing a subsequence of the hammerhead ribozyme (U7−A14) was efficiently cleaved (see below) and enabled further characterization of the cleavage products. Because of the short 5′-fragments formed after cleavage, the 2′,3′-cyclic phosphate could be separated from the open phosphate by gel electrophoresis and revealed that the major product was the 2′,3′-cyclic phosphate (data not shown).

Rate of Zn^{2+}-Promoted Cleavage. The ribozyme−substrate complex was incubated at 37 °C in the presence and absence of 100 μM Zn^{2+}, and the reaction mixtures were analyzed by DPAGE. To measure the rate dependence of pH, the incubation was performed at different pH values (5.6−9.1) for 72−264 h. The longer reaction times were required for lower pH values. The data for a time course experiment (at pH 7.1) are shown in Figure 3A. Cleavage between G8 and A9 was specific and extensive, compared to the control (no added Zn^{2+}) in which no detectable cleavage was observed. The extent of cleavage between G8 and A9 was determined by densitometry analysis. As seen in Figure 3B, depletion of the full-length ribozyme is concomitant with formation of the 5′ product. Also apparent is that the sum of the full-length ribozyme and the 5′ product is not 100% after incubation for a long period of time. This is due to nonspecific cleavage at sites other than between G8 and A9 (see below).

To determine the rate of the unimolecular cleavage reaction, the logarithm of the percent ribozyme remaining was plotted as a function of time. One example is shown in Figure 4A, for the reaction at pH 7.1. The negative slope of the least-squares plot yielded the reaction rate of 2.9×10^{-4} min^{-1}. Inclusion of the noncleavable substrate was not required for efficient cleavage between G8 and A9. In fact, a subsequence of the hammerhead ribozyme (U7−A14) also showed efficient cleavage. The rates of hammerhead ribozyme cleavage with and without substrate and the U7−A14 sequence were compared at pH 7.6 and found to be 5.9×10^{-4}, 4.9×10^{-4}, and 3.9×10^{-4} min^{-1}, respectively.

The cleavage rates were determined at different pH values. A plot of the logarithm of the reaction rates as a function of pH (Figure 4B) revealed a linear relationship at lower pH values, up to ca. pH 8.3. It should also be noted that we observed minor cleavage in the U-turn of the hammerhead ribozyme (between C3 and U4) above pH 7.5. To verify that the decrease in rate at the higher pH values was not due to precipitation of zinc hydroxide, the concentration of Zn^{2+} was determined by atomic absorption spectroscopy (data not shown). These measurements were conducted at 22 °C, and

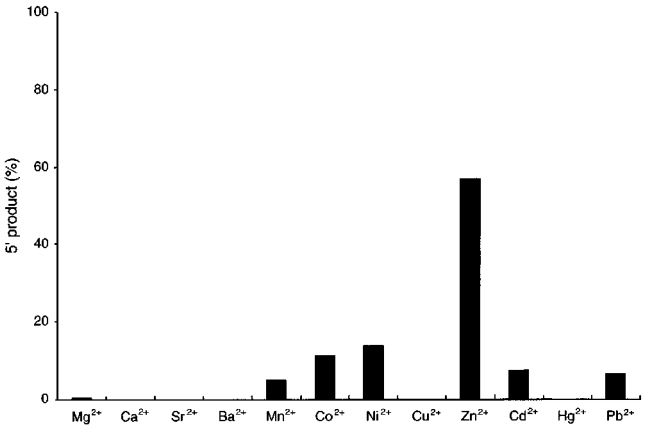

FIGURE 5: Extent of cleavage of the hammerhead ribozyme for different divalent metal ions. Conditions (37 °C, 24 h): 50 mM Tris, pH 8.6, 200 mM NaCl, 10 μM Na_2EDTA, 2 μM substrate, <300 nM ribozyme, 20 μM $M(OAc)_2$.

all solutions were found to contain 100 μM Zn^{2+}, except at the highest pH (pH 9.4 at 22 °C, CHES buffer), where the concentration was 30 μM. However, when this solution was warmed to 37 °C (pH 9.1), the temperature at which the cleavage experiments were performed, the Zn^{2+} concentration in solution was determined to be 100 μM.

The rate of nonspecific, Zn^{2+}-promoted cleavage was determined at pH 7.1 by two different methods. First, the logarithm of the sum of remaining ribozyme and the amount of the Zn^{2+} cleavage product at position A9 was plotted as a function of time. This yielded the rate constant, which was normalized to a single phosphodiester by dividing by 36, the number of phosphodiesters other than A9 in the hammerhead ribozyme. These calculations yielded a rate constant of 7.6×10^{-7} min^{-1}, which is ca. 400-fold lower that than observed for the specific cleavage at A9. The second method involved treating the chimeric oligomer 5′-CGA ACT CAC TAT (rA)GG AAG AGA TG, containing deoxynucleotides with the exception of a single ribonucleotide (*23*), under the same conditions as the hammerhead ribozyme, at pH 7.7. The rate of cleavage of the chimera was found to be 5.0×10^{-6} min^{-1}, 90-fold slower than for A9 cleavage (4.6×10^{-4} min^{-1} at pH 7.7). These experiments show that the rate of cleavage between G8 and A9 is between 2 and 3 orders of magnitude higher than for the background cleavage.

Divalent Metal Ion Specificity. To determine the metal ion specificity of the cleavage observed between G8 and A9, the hammerhead ribozyme−substrate complex was incubated with a variety of different divalent metal ions (20 μM) at pH 8.6 for 24 h. Analysis of these reactions revealed that Zn^{2+} shows the most extensive cleavage (57%) of the metal ions tested (Figure 5). Ni^{2+} and Co^{2+} yielded 12 and 14% cleavage, respectively, while Mn^{2+}, Cd^{2+}, and Pb^{2+} gave between 5 and 8% cleavage. Negligible cleavage was observed in the presence of the alkaline-earth metal ions. When this experiment was conducted at pH 7.5, the same trend was observed, except for Pb^{2+}, where cleavage was almost as efficient (23%) as for Zn^{2+} (26%). It is not clear why the Pb^{2+}-promoted cleavage was significantly lower at pH 8.6. Atomic absorption spectroscopy measurements showed that it was not due to precipitation of lead hydroxide (data not shown). A competition experiment was also performed at pH 8.1, in which the ribozyme was incubated with different concentrations of Mg^{2+} for 10 min, followed by addition of Zn^{2+} to a final concentration of 100 μM and incubation at 37 °C for 24 h. No change in the amount of cleavage was observed for up to 100 μM Mg^{2+} (57% cleavage), but the extent of cleavage was gradually reduced at 1 mM, 10 mM, and 100 mM to 47%, 23%, and 6%, respectively.

Effect of Monovalent Ions on Cleavage. The most efficient Zn^{2+}-dependent cleavage was observed at 0.5 M concentrations of monovalent ions where 56% cleavage was observed for Na^+ and 33.8% for Li^+. It should be noted that cleavage was reduced to 19.5% in the absence of monovalent ions, presumably because they stabilize the secondary structure required for the formation of the cleavage site. High (>1 M) concentrations of Na^+ or Li^+ drastically reduced the extent of cleavage. However, Zn^{2+}-dependent cleavage could not be completely suppressed even at very high concentration of monovalent ions (4 M, extent of cleavage 0.9% for Li^+ and 5.8% for Na^+). No cleavage was detected in the absence of divalent metal ions, even at monovalent ion concentrations of 4 M, where the hammerhead ribozyme has been shown to catalyze substrate cleavage (*5*, *7*, *8*).

DISCUSSION

Despite much study devoted to metal ion−hammerhead ribozyme interactions, specifically the A9/G10.1 metal ion binding site, divalent metal ion-promoted cleavage between the neighboring nucleotides G8 and A9, has gone unnoticed. This is possibly due to the fact that many metal ion−hammerhead experiments involve only a ^{32}P-labeled substrate, rendering the cleaved ribozyme unobservable, in addition to the longer incubation required to observe significant cleavage between G8 and A9.

For studies of the cleavage reaction between nucleotides G8 and A9, we chose the kinetically and structurally well-studied HH16 construct (Figure 1) (*24*). This ribozyme construct forms a stable complex with its substrate and is not prone to misfolding. A noncleavable substrate, containing deoxycytidine in place of cytidine at the traditional cleavage site, was used in our initial experiments. However, it was subsequently determined that exclusion of the noncleavable substrate had a minor effect on the rate of cleavage, indicating that the metal ion binding site formed without substrate. Furthermore, incubation of a short oligomer containing the subsequence U7−A14 of the hammerhead ribozyme cleaved with a similar rate to that observed with the full ribozyme. These data show that cleavage at the G8/A9 site does not rely on the tertiary structure of this ribozyme, which is required for substrate cleavage. This is consistent with NMR experiments that have located a metal ion bound to G-A mismatches of RNA duplexes such as those found as an extension of helix II in the hammerhead ribozyme (*25*).

Previously described small RNA cleavage motifs that do not rely on complex tertiary interactions include the leadzyme (*26*) and the Mn^{2+}-dependent ribozyme (*27*). These ribozymes have mechanistic similarities to the cleavage activity described here: all require divalent metal ions for activity, and the RNA is cleaved by the attack of a 2′-hydroxyl group on the adjacent phosphodiester. The Mn^{2+}-dependent motif bears a strong resemblance to the Zn^{2+}-

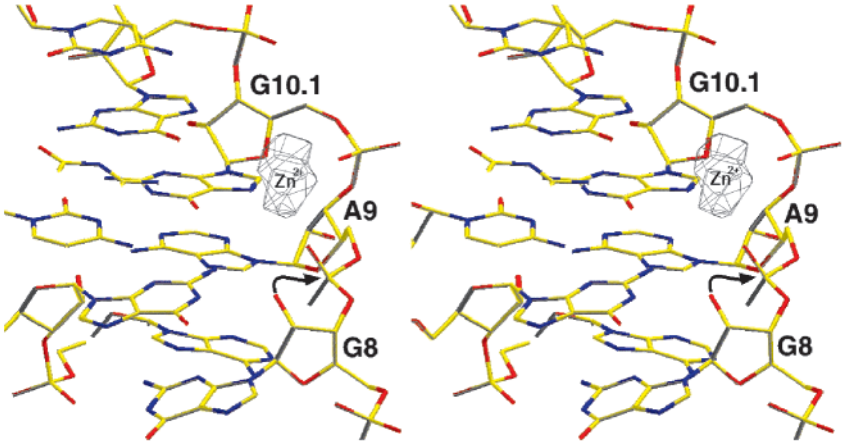

FIGURE 6: Stereo image of the crystal structure of the A9/G10.1 metal ion binding site in the presence of Zn^{2+}. The difference density shows the position of the Zn^{2+} ion, and the arrow shows the attack of the 2′-hydroxyl group on the scissile phosphate. The hammerhead ribozyme sequence, crystallization, and data collection were as previously described (*12*). These data had an $R_{scale} = 0.077$ with $I/\sigma I = 12.3$ and a redundancy of 3.1. One hammerhead ribozyme molecule and 9 Zn^{2+} atoms were refined in the asymmetric unit of the crystal using 8291 of 8606 reflections $>2\sigma$ with a completeness of 94.29% using standard simulated annealing protocols in X-PLOR. The crystallographic *R*-factors were 0.281 (R_{free}) and 0.247 (R_{test}), with rmsd bond lengths = 0.010 Å and rmsd bond angles = 1.58°. All atoms placed within the crystallographic asymmetric unit had an occupancy of 1.00.

dependent cleavage of the U7−A14 sequence because cleavage occurs near a helical end and generates a 2′,3′-cyclic phosphate. The sequence requirement for the Mn^{2+} cleavage is GAAA (*28*) whereas the U7−A14 sequence contains a pair of G-A mismatches, although the full sequence requirement for the latter has not been systematically explored.

We initially observed specific cleavage between G8 and A9 in control experiments where the divalent metal ion was left out. This background cleavage was suppressed with EDTA, indicating that the cleavage-causing impurity was a divalent or a trivalent metal ion, possibly a contaminant in the buffer or NaCl used in the experiments. It is noteworthy that high concentrations of NaCl often contain significant heavy-metal impurities (1 M NaCl = <20 μM heavy metals), even using the purest commercially available chemicals. This is an important fact to keep in mind when incubating RNAs in solutions that have high concentrations of salts or buffers.

The rate of Zn^{2+}-dependent cleavage between G8 and A9 was determined to be 3.0×10^{-4} min^{-1} at pH 7.1, which is ca. 3 orders of magnitude slower than hammerhead-mediated substrate cleavage in the presence of 10 mM Mg^{2+} (*24*). The rate of nonspecific Zn^{2+}-dependent cleavage in the hammerhead ribozyme was ca. 400-fold slower than that observed with the G8/A9 cleavage. To determine the upper limit for the rate of nonspecific background cleavage, we used a chimeric oligonucleotide, which contained only one ribonucleotide (*23*). The lack of unimolecular or bimolecular secondary structures in this oligomer allows it to readily attain the conformation required for cleavage by an in-line mechanism by the attack of the 2′-hydroxyl group on the scissile phosphate. This conformation is not present in A-form duplex RNA, which is found in the helices of the hammerhead ribozyme. Therefore, the rate of background cleavage was expected to be higher for the chimera. Indeed, the rate of cleavage for the chimera was 3-fold higher than the rate of background cleavage for the hammerhead ribozyme.

A plot of the logarithm of the rate as a function of pH revealed a linear dependence (Figure 4B) which is indicative of proton loss in the cleavage mechanism, either prior to or in the rate-determining step (*6*). The rate increased linearly up to ca. pH 8.3, suggesting that the proton being transferred in the Zn^{2+}-promoted cleavage reaction has a pK_a of ca. 8.3. In fact, this pK_a is close to that of the aqua complex of Zn^{2+} [pK_a = 9.0 (*29*)]. It is possible that the pK_a of a water ligand of the Zn^{2+} complex at the A9/G10.1 metal ion binding site is lowered to 8.3 by the other ligands; for example, complexes of Zn^{2+} have been observed with pK_as as low as 7.5 (*30*). If the pK_a of the A9/G10.1-bound zinc hydroxide is 8.3, one interpretation of our data is that it is acting as a general base in the cleavage reaction. Taken together with the fact that the products of the reaction are a free 5′-hydroxyl group and a 2′,3′-cyclic phosphate, we postulate that a zinc hydroxide complex abstracts the proton from the 2′-hydroxyl group of G8, which attacks the A9 phosphate and initiates cleavage.

Several crystal structures have been solved of the hammerhead ribozyme (*9*−*12*), including one in the presence of Zn^{2+}, which was observed bound to the A9/G10.1 metal ion binding site (Figure 6) (*12*). Interestingly, inspection of the metal binding site reveals that the 2′-hydroxyl group of G8 is positioned for a nucleophilic in-line attack on the scissile phosphate, which initializes transesterification and phosphodiester bond cleavage. This is the same conformation as observed in the presence of other divalent metal ions, such as Mg^{2+}, which is not able to induce cleavage. Thus, it may not suffice to induce a conformational change that orients a nucleophile for a reaction with an electrophile as a general catalytic strategy. Specifically, it is not sufficient to attain the conformation required for an in-line attack of the 2′-hydroxyl of G8 on the adjacent phosphodiester for efficient catalysis.

Given the fact that G8 is in a conformation that is conducive to cleavage, we investigated which metal ions were able to support this cleavage. No cleavage was observed with the monovalent ions Na^+ and Li^+, even at 4 M concentration. The alkaline-earth metals Mg^{2+}, Ca^{2+}, Ba^{2+}, and Sr^{2+} showed negligible detectable cleavage at pH 8.6, and the transition-metal ions Mn^{2+}, Cd^{2+}, Pb^{2+}, Ni^{2+}, and Co^{2+} showed

significantly less cleavage than Zn^{2+} (Figure 5), although Pb^{2+} showed almost as much cleavage as Zn^{2+} at pH 7.5. These experiments were performed at relatively low concentration of metal ions (20 μM). In an attempt to demonstrate that the metal ion binding site was saturated, the metal ion concentration was varied up to 10 mM concentration (data not shown). Extensive nonspecific cleavage was observed for many of the metal ions at higher concentrations, which precluded determination of the equilibrium dissociation constants. However, some of the metal ions showed increased specific cleavage at higher concentrations, indicating that the experiment was performed under subsaturating conditions. For example, Cu^{2+} showed ca. 0.3% and 9% cleavage at 20 μM and 10 mM concentration, respectively.

The Zn^{2+}-dependent cleavage was gradually reduced upon titration of Mg^{2+}, Na^{+}, or Li^{+} into the sample, but an appreciable decrease in the cleavage was observed only at high concentrations of the inhibitory ions. The simplest interpretation of the titration experiment is that Mg^{2+}, Na^{+}, or Li^{+} can compete with Zn^{2+} for binding at the A9/G10.1 site. However, we cannot rule out the possibility that the inhibitory ions are stabilizing an alternate conformation that either has lower affinity for Zn^{2+} or has a lower rate of cleavage due to structural distortion.

Why is Zn^{2+} such an effective cofactor for cleavage at the G8/A9 position? There are at least four factors that can affect the efficiency of a metal ion cofactor for cleavage at the G8/A9 site. First, the identity of ligands at the A9/G10.1 site will modulate its affinity to the metal ions, which is important to keep in mind because the metal ion experiment was performed at subsaturating concentration of metal ions. For example, Zn^{2+} is a hard Lewis acid and thus has a high affinity for hard Lewis bases, such as the *pro-*R_P phosphate oxygen of A9 and N7 of G10.1. The high affinity of Zn^{2+} for the A9/G10.1 site is reflected by the experimental observation that Zn^{2+}-dependent cleavage could not be completely suppressed with 100 mM Mg^{2+}. Second, the pK_a of the metal ion hydroxide is important, assuming that it is involved in the abstraction of the 2′-hydroxyl proton. The pK_as of the aqua complexes of Mn^{2+} and the alkaline-earth metals are all high (10−13) and will therefore not have a significant concentration of the corresponding metal hydroxide at the pH values at which the experiments were conducted. On the other hand, the pK_as of the aqua complexes of Cd^{2+}, Ni^{2+}, Co^{2+}, Pb^{2+}, and Zn^{2+} fall within the 7−10 range (*31*). This fact may contribute to the previously observed nonspecific Zn^{2+}-dependent hydrolysis of RNA (*32*−*34*). Third, the geometric requirements of the binding site place a limitation on the size of the bound metal ion. However, this factor is probably not relevant here because Pb^{2+}, with the large ionic radius of 1.3 Å, yields significant cleavage at pH 7.5. The other divalent metal ions that catalyze cleavage have ionic radii of approximately 0.7 Å (*35*). Finally, the coordination geometry of the metal complex at the A9/G10.1 site may influence the placement of the metal-bound hydroxide close to the 2′-hydroxyl group of G8 at the cleavage site. Unlike most of the other metal ions, Zn^{2+} prefers tetrahedral geometry, and it is possible that coordination of a water molecule to the Zn^{2+} ion with a tetrahedral geometry could place it in the vicinity of the cleavage site. However, the resolution of the crystal structure is not high enough to unambiguously place the general base.

Although the conformation at the cleavage site is conducive to in-line attack of the 2′-hydroxyl of G8 on the scissile phosphate and a general base is placed in the vicinity of the 2′-hydroxyl group, it is noteworthy that the rate of cleavage is 3−4 orders of magnitude lower than that observed for most ribozymes. It has been suggested that the orientation of the orbitals involved in the cleavage reaction may be an important factor for efficient cleavage of RNA (*36*). Another possible explanation for this relatively low activity is that the general base might not be optimally positioned for abstracting the proton from the 2′-hydroxyl group. These results could also reflect the importance of leaving group stabilization by a Lewis acid, like the metal ion at the catalytic sites of group I introns (*37*). Thus, the 2−3 orders of magnitude rate-acceleration over the background cleavage observed here could indicate that a similar rate-enhancement might be expected for a strategically placed Lewis acid.

Techniques that identify metal ion binding sites in RNA are valuable, given the importance of divalent metal ions in RNA function. Several different approaches have been developed for this purpose. One example is the incorporation of phosphorothioates (*38*), which have low affinity for hard metals (e.g., Mg^{2+}) but high affinity for soft metals (e.g., Mn^{2+}), in combination with a functional assay. Spectroscopic methods, such as solution NMR (*14*, *39*, *40*) and EPR (*41*−*43*), have been used to directly detect metal ion binding. Metal ion-induced RNA cleavage has been used to identify metal ion binding sites, such as Pb^{2+} (*44*, *45*), Tb^{3+} (*46*−*48*), and uranyl photocleavage (*49*, *50*). Our work suggests that it may be advantageous to incubate RNA with a number of different metal ions when searching for metal ion binding sites by metal-ion promoted RNA cleavage. For example, uranyl cleavage of the hammerhead ribozyme did not show cleavage at the G8/A9 site; rather, cleavage was observed at another metal ion binding site (G5) (*50*). In addition to identifying metal ion binding sites, metal ion cleavage can be a useful probe of function under different conditions and has been used to study the folding of RNA (*51*, *52*).

In conclusion, we have described a new divalent metal ion-dependent RNA cleavage motif, found in the hammerhead ribozyme. This cleavage activity does not require the full-length sequence of the hammerhead ribozyme and is the first example of a metalloribozyme that shows preference for Zn^{2+} ions, although in vitro selection techniques have been used to select Zn^{2+}-dependent deoxyribozymes (*53*). To our knowledge, the crystal structure of this cleavage site (*12*) is the first structure of an RNA catalytic site that shows the correct conformation for RNA cleavage, along with the required catalytic group.

ACKNOWLEDGMENT

We thank Dr. M. Sadilek for help with mass spectrometry analyses, Dr. J. Roe for atomic spectroscopy, and Dr. F. Eckstein and the Sigurdsson Research Group for critical review of the manuscript. We also thank Dr. W. G. Scott for providing the refined crystal structure of the hammerhead ribozyme in the presence of Zn^{2+} (Figure 6) and for valuable discussions.

REFERENCES

1. Sigurdsson, S. T., Thomson, J. B., and Eckstein, F. (1998) in *RNA Structure and Function*, pp 339−375, Cold Spring Harbor Laboratory Press, Cold Spring Harbor, NY.

2. Dahm, S. C., and Uhlenbeck, O. C. (1991) *Biochemistry 30*, 9464−9469.
3. Koizumi, M., and Ohtsuka, E. (1991) *Biochemistry 30*, 5145−5150.
4. Slim, G., and Gait, M. J. (1991) *Nucleic Acids Res. 19*, 1183−1188.
5. Murray, J. B., Seyhan, A. A., Walter, N. G., Burke, J. M., and Scott, W. G. (1998) *Chem. Biol. 5*, 587−595.
6. Dahm, S. C., Derrick, W. B., and Uhlenbeck, O. C. (1993) *Biochemistry 32*, 13040−13045.
7. Curtis, E. A., and Bartel, D. P. (2001) *RNA 7*, 546−552.
8. O'Rear, J. L., Wang, S., Feig, A. L., Beigelman, L., Uhlenbeck, O. C., and Herschlag, D. (2001) *RNA 7*, 537−545.
9. Pley, H. W., Flaherty, K. M., and McKay, D. B. (1994) *Nature 372*, 68−74.
10. Scott, W. G., Finch, J. T., and Klug, A. (1995) *Cell 81*, 991−1002.
11. Scott, W. G., Murray, J. B., Arnold, J. R. P., Stoddard, B. L., and Klug, A. (1996) *Science 274*, 2065−2069.
12. Murray, J. B., Terwey, D. P., Maloney, L., Karpeisky, A., Usman, N., Beigelman, L., and Scott, W. G. (1998) *Cell 92*, 665−673.
13. Feig, A. L., Scott, W. G., and Uhlenbeck, O. C. (1998) *Science 279*, 81−84.
14. Hansen, M. R., Simorre, J. P., Hanson, P., Mokler, V., Bellon, L., Beigelman, L., and Pardi, A. (1999) *RNA 5*, 1099−1104.
15. Ruffner, D. E., and Uhlenbeck, O. C. (1990) *Nucleic Acids Res. 18*, 6025−6029.
16. Nakamatsu, Y., Warashina, M., Kuwabara, T., Tanaka, Y., Yoshinari, K., and Taira, K. (2000) *Genes Cells 5*, 603−612.
17. Peracchi, A., Beigelman, L., Scott, E. C., Uhlenbeck, O. C., and Herschlag, D. (1997) *J. Biol. Chem. 272*, 26822−26826.
18. Wang, S., Karbstein, K., Peracchi, A., Beigelman, L., and Herschlag, D. (1999) *Biochemistry 38*, 14363−14378.
19. Murray, J. B., and Scott, W. G. (2000) *J. Mol. Biol. 296*, 33−41.
20. Greig, M., and Griffey, R. H. (1995) *Rapid Commun. Mass Spectrom. 9*, 97−102.
21. Dharmacon Research (1999) Technical Bulletin #001.
22. Luce, R. A., Sigurdsson, S. T., and Hopkins, P. B. (1999) *Biochemistry 38*, 8682−8690.
23. Li, Y. F., and Breaker, R. R. (1999) *J. Am. Chem. Soc. 121*, 5364−5372.
24. Hertel, K. J., Herschlag, D., and Uhlenbeck, O. C. (1994) *Biochemistry 33*, 3374−3385.
25. Tanaka, Y., Morita, E. H., Hayashi, H., Kasai, Y., Tanaka, T., and Taira, K. (2000) *J. Am. Chem. Soc. 122*, 11303−11310.
26. Pan, T., and Uhlenbeck, O. C. (1992) *Nature 358*, 560−563.
27. Dange, V., Van Atta, R. B., and Hecht, S. M. (1990) *Science 248*, 585−588.
28. Kazakov, S., and Altman, S. (1992) *Proc. Natl. Acad. Sci. U.S.A. 89*, 7939−7943.
29. Perrin, D. D. (1962) *J. Chem. Soc.*, 4500−4502.
30. Zompa, L. J. (1978) *Inorg. Chem. 17*, 2531−2536.
31. Burgess, J. (1978) *Metal ions in solution*, Ellis Horwood Limited, Sussex, U.K.
32. Butzow, J. J., and Eichhorn, G. L. (1971) *Biochemistry 10*, 2019−2027.
33. Kuusela, S., and Lonnberg, H. (1994) *J. Chem. Soc., Perkin Trans. 2*, 2301−2306.
34. Kaukinen, U., Bielecki, L., S., M., Adamiak, R. W., and Lonnberg, H. (2001) *J. Chem. Soc., Perkin Trans. 2*, 1024−1031.
35. Kleinberg, J., Argersinger, W. J., and Griswold, E. (1960) *Inorganic Chemistry*, D. C. Heath and Co., Boston, MA.
36. Scott, W. G. (2001) *J. Mol. Biol. 311*, 989−999.
37. Piccirilli, J. A., Vyle, J. S., Caruthers, M. H., and Cech, T. R. (1993) *Nature 361*, 85−88.
38. Eckstein, F. (1985) *Annu. Rev. Biochem. 54*, 367−402.
39. Butcher, S. E., Allain, F. H. T., and Feigon, J. (2000) *Biochemistry 39*, 2174−2182.
40. Maderia, M., Hunsicker, L. M., and DeRose, V. J. (2000) *Biochemistry 39*, 12113−12120.
41. Horton, T. E., Clardy, D. R., and DeRose, V. J. (1998) *Biochemistry 37*, 18094−18101.
42. Morrissey, S. R., Horton, T. E., Grant, C. V., Hoogstraten, C. G., Britt, R. D., and DeRose, V. J. (1999) *J. Am. Chem. Soc. 121*, 9215−9218.
43. Morrissey, S. R., Horton, T. E., and DeRose, V. J. (2000) *J. Am. Chem. Soc. 122*, 3473−3481.
44. Brown, R. S., Hingerty, B. E., Dewan, J. C., and Klug, A. (1983) *Nature 303*, 543−546.
45. Winter, D., Polacek, N., Halama, I., Streicher, B., and Barta, A. (1997) *Nucleic Acids Res. 25*, 1817−1824.
46. Walter, N. G., Yang, N., and Burke, J. M. (2000) *J. Mol. Biol. 298*, 539−555.
47. Hargittai, M. R. S., and Musier-Forsyth, K. (2000) *RNA 6*, 1672−1680.
48. Sigel, R. K. O., Vaidya, A., and Pyle, A. M. (2000) *Nat. Struct. Biol. 7*, 1111−1116.
49. Mollegaard, N. E., Murchie, A. I. H., Lilley, D. M. J., and Nielsen, P. E. (1994) *EMBO J. 13*, 1508−1513.
50. Bassi, G. S., Mollegaard, N. E., Murchie, A. I., von Kitzing, E., and Lilley, D. M. (1995) *Nat. Struct. Biol. 2*, 45−55.
51. Ciesiolka, J., Hardt, W. D., Schlegl, J., Erdmann, V. A., and Hartmann, R. K. (1994) *Eur. J. Biochem. 219*, 49−56.
52. Brannvall, M., Mikkelsen, N. E., and Kirsebom, L. A. (2001) *Nucleic Acids Res. 29*, 1426−1432.
53. Li, J., Zheng, W., Kwon, A. H., and Lu, Y. (2000) *Nucleic Acids Res. 28*, 481−488.

BI015634C